J Neurophysiol 107: 2958–2970, 2012.
First published February 29, 2012; doi:10.1152/jn.01028.2011.

$GABA_A$ receptors increase excitability and conduction velocity of cerebellar parallel fiber axons

Shlomo S. Dellal,* Ray Luo,* and Thomas S. Otis
Department of Neurobiology, David Geffen School of Medicine, University of California, Los Angeles, California

Submitted 9 November 2011; accepted in final form 27 February 2012

Dellal SS, Luo R, Otis TS. $GABA_A$ receptors increase excitability and conduction velocity of cerebellar parallel fiber axons. *J Neurophysiol* 107: 2958–2970, 2012. First published February 29, 2012; doi:10.1152/jn.01028.2011.—In the adult mammalian brain, $GABA_A$ receptors ($GABA_A$Rs) are responsible for the predominant forms of synaptic inhibition, but these receptors can excite neurons when the chloride equilibrium potential (E_{Cl}) is depolarized. In many mature neurons, $GABA_A$Rs are found on presynaptic terminals where they exert depolarizing effects. To understand whether excitatory GABA action affects axonal function, we used transverse cerebellar slices to measure the effects of photolysis of caged GABA on the initiation and propagation of compound parallel fiber (PF) action potentials (APs). Photolysis of caged GABA increased the amplitude and conduction velocity of PF APs; GABA reuptake blockers and a positive modulator of $GABA_A$Rs enhanced these effects. In contrast, a modulator selective for δ-subunit-containing $GABA_A$Rs did not enhance these effects and responsiveness remained in $\delta^{-/-}$ mice, arguing that δ-subunit-containing $GABA_A$Rs are not required. Synaptically released GABA also increased PF excitability, indicating that the mechanism is engaged by physiological signals. A Hodgkin-Huxley-style compartmental model of the PF axon and granule cell body was constructed, and this model recapitulated the GABA-dependent decrease in AP threshold and the increase in conduction velocity, features that were sensitive to E_{Cl} and to the voltage dependence of sodium channel inactivation. The model also predicts that axonal $GABA_A$Rs could affect orthodromic spike initiation. We conclude that GABA acting on cerebellar PFs facilitates both spike generation and propagation, allowing axons of granule cells to passively integrate signals from inhibitory interneurons and influence information flow in the input layer to the cerebellar cortex.

γ-aminobutyric acid; presynaptic modulation; axonal excitability; δ-subunit; fiber volley; caged γ-aminobutyric acid

THE CLASSICAL STUDIES OF MUSCLE afferent inputs to spinal motor neurons that gave rise to the concept of presynaptic inhibition also eventually led to the first identification of presynaptic $GABA_A$ receptors ($GABA_A$Rs) (Eccles et al. 1963). Subsequent work by many laboratories demonstrated that this $GABA_A$R-mediated presynaptic inhibition results from a depolarizing action of GABA on presynaptic afferent terminals (Rudomin and Schmidt 1999). Since those initial findings, $GABA_A$Rs have been observed on presynaptic terminals in a variety of brain regions, including auditory brain stem, ventral tegmental area, hypothalamus, amygdala, hippocampus, cerebellum, and cortex, and in most of these locations GABA has been found to be depolarizing (Alle and Geiger 2007; Khirug et al. 2008; Pugh and Jahr 2011; Stell et al. 2007; Szabadics et al. 2006; Trigo et al. 2007; Turecek and Trussell 2002; Woodruff et al. 2006; Xiao et al. 2007; Zhang and Jackson 1993). Cell-attached and perforated patch-clamp approaches applied to large axon terminals in brain stem auditory nuclei, anterior pituitary, and hippocampus have indicated that depolarizing effects of GABA can be attributed to a depolarized chloride equilibrium potential (E_{Cl}) (Price and Trussell 2006; Ruiz et al. 2010; Zhang and Jackson 1993).

Although there have been many studies on the consequences of presynaptic $GABA_A$Rs on synaptic transmission, relatively little is known about whether these receptors affect axonal excitability. To directly test whether transient activation of $GABA_A$R affects axonal excitability, we have taken advantage of transverse cerebellar slices, which preserve PF axons, allowing compound action potentials (APs) to be recorded as fiber volleys. Prior studies of GABA action on parallel fiber (PFs) have established that activation of axonal $GABA_A$Rs increases the frequency of synaptic currents recorded in postsynaptic targets of PFs (Stell et al. 2007). This increased excitability is accompanied by increases in calcium transients in PF axonal bundles (Stell 2011) and in single en passant PF synaptic boutons (Pugh and Jahr 2011). Electron microscopy data have demonstrated that $GABA_A$R subunits are present on PF presynaptic boutons and likely on axons, as well (Stell et al. 2007). The experiments presented here extend this work to examine how $GABA_A$Rs affect axonal excitability.

We have found that UV photolysis of GABA, α-carboxy-2-nitrobenzyl ester (CNB-caged GABA) increases both the amplitude and conduction velocity of PF volleys, effects that are inhibited by $GABA_A$R antagonists, enhanced by blocking GABA reuptake, and enhanced by broad spectrum modulators of $GABA_A$Rs. Trains of stimuli generate increases in axonal excitability that are blocked by $GABA_A$R antagonists and enhanced by GABA reuptake inhibitors, suggesting that these mechanisms are engaged by physiological activity. Recognizing the prominent extrasynaptic $GABA_A$R conductance present in granule cell bodies, we tested whether $GABA_A$R-mediated excitation of PFs persists in δ-subunit knockout mice and found no differences from wild type, indicating that extrasynaptic $GABA_A$Rs composed with this subunit are not required.

Construction of a compartmental model of the PF axon and granule cell body allowed us to examine the effects of different chloride gradients in the axon. With a depolarized E_{Cl}, the model reproduced the GABA-dependent decrease in spike initiation threshold and increase in conduction velocity. The magnitude of E_{Cl} relative to the resting potential and the voltage dependence of sodium channel inactivation were critical factors in the model behavior. The model indicated that PF axons could act like

* S. S. Dellal and R. Luo contributed equally to this work.

Address for reprint requests and other correspondence: T. S. Otis, Dept. of Neurobiology, David Geffen School of Medicine at UCLA, Los Angeles, CA 90095 (e-mail: otist@ucla.edu).

dendrites to passively integrate $GABA_A$R-mediated depolarization and influence AP initiation at the spike initiation zone.

Together these observations show that depolarizing $GABA_A$Rs can robustly influence the electrical behavior of axons. Interestingly, the GABA- and activity-induced increases in excitability that we describe here show many similarities to a phenomenon termed "supernormal excitability," identified in PF axons in vivo (Gardner-Medwin 1972; Malenka et al. 1983). Our results suggest that $GABA_A$Rs contribute to this activity-induced increase in conduction velocity and excitability and that this mechanism allows molecular layer inhibitory interneurons to influence the timing and strength of information emanating from the granule cell layer, the principal input layer of the cerebellum.

MATERIALS AND METHODS

Brain slice electrophysiology. After deep anesthesia was induced with isoflurane, mice were decapitated, in accordance with a protocol approved by the University of California, Los Angeles Institutional Animal Care and Use Committee. The cerebellum vermis was removed and placed in an ice-cold cutting solution containing (in mM) 85 NaCl, 2.5 KCl, 0.5 $CaCl_2$, 4 $MgCl_2$, 1.25 NaH_2PO_4, 24 $NaHCO_3$, 25 glucose, and 75 sucrose. Transverse slices (300 μm) were cut from 19- to 35-day-old C57/Bl6 wild-type or $\delta^{-/-}$ mice with a Leica VT1000 vibratome (Leica Microsystems, Wetzlar, Germany) and stored in external recording solution containing (in mM) 119 NaCl, 2.5 KCl, 2 $CaCl_2$, 1 $MgCl_2$, 1 NaH_2PO_4, 26.2 $NaHCO_3$, and 25 glucose, warmed to 35°C for 15–20 min, after which the solution was allowed to reach room temperature. All solutions were continuously bubbled with 95% O_2-5% CO_2. All drugs and reagents were purchased from Sigma-Aldrich (St. Louis, MO), Tocris Bioscience (Ellisville, MO), Ascent Scientific (Princeton, NJ), or Invitrogen (Carlsbad, CA). Recordings were made at room temperature with a Dagan BVC-700A (Dagan, Minneapolis, MN), Axopatch 200A, or Axopatch 200B amplifier (Axon Instruments, Foster City, CA). Data was acquired with pClamp software (Axon Instruments).

External solutions during recordings contained CGP-35348 (100 μM) to block $GABA_B$ receptors and *O*-(CNB-caged) GABA (100 μM) in the photolysis experiments. CGP 35348 (100 μM) was also included in the stimulus train experiments. All experiments were conducted at room temperature and under recirculation of the external solution (7–10 ml total volume) at a flow rate of 2–4 ml/min. Extracellular population spike (fiber volley) recordings were carried out as follows. A bipolar stimulating electrode (FHC, Bowdoin, ME) was placed in the molecular layer, and a recording electrode (1–3 MΩ) was placed in the same molecular layer 80–500 μm distal to the stimulating electrode. Single stimuli ranging in duration from 40 to 400 μs and in intensity from 15 to 350 μA were delivered to the stimulating electrode via an Iso-Flex stimulator (A.M.P.I., Jerusalem, Israel) to elicit the fiber volley. All fiber volleys were AP-dependent, since they were eliminated by TTX (0.5–1 μM).

Photolysis of caged GABA. Photolysis of caged GABA was accomplished with a 2-s UV flash from an epifluorescence lamp using a 366-nm center wavelength, full-width half-maximum 17-nm excitation filter, a 409-nm dichroic mirror (both filters from Semrock, Rochester, NY), and either a ×40, N.A. 0.8 or ×60, N.A. 0.9 objective, as described previously (Dittman and Regehr 1997), and was shuttered by a digital pulse from a Master-8 interval generator (A.M.P.I.).

A prior study that used photolysis of 150 μM CNB-caged GABA in transverse cerebellar slices estimated a peak GABA concentration of ~10 μM (Dittman and Regehr 1997). Although similar in many respects to our experiments (same preparation, same objective lens, same caged GABA at a similar concentration), this study used a different UV source (flash lamp rather than an arc lamp) and applied GABA locally to the slice, reducing extinction effects caused by UV absorption of caged GABA when it is circulating in the bath. Nonetheless, their estimates are consistent with maximal peak concentrations in the range of tens of micromolar at the slice surface. Given the high UV absorption of cerebellar tissue (DiGregorio et al. 2007), it is expected that progressively lower concentrations would be achieved with depth in the slice.

UV light has been reported to have direct effects on many ion channels including $GABA_A$ receptors (Chang et al. 2001). With this in mind, we performed a number of control experiments, including testing the effects of UV light pulses in the absence of caged GABA, testing UV pulses with $GABA_A$ receptor antagonists present (see Fig. 1), and testing the effects of endogenous GABA (see Fig. 8). These experiments confirmed that UV-induced transient potentiation of fiber volleys and of conduction velocity were dependent on both the presence of caged GABA and functional $GABA_A$Rs.

Endogenous GABA excitation. To elicit endogenous GABA release, 20-Hz stimulus trains were delivered for 1.5–3 s. Stimulus intensity (100–200 μA, 40–150 μs) was fixed throughout a single experiment, and all experiments were conducted in the $GABA_B$R blocker CGP-35348 (100 μM). Using a blinded experimental design, we compared the effects of control solution with a solution containing 100 μM CdCl. In each experimental group, picrotoxin (PTX; 100 μM) was applied to isolate the PTX-sensitive response to the train.

Experiments examining the effects of NNC-711 (10 μM) were not blinded. In these experiments NNC-711 was applied, followed by PTX, allowing the PTX-sensitive responses to be calculated for both control and NNC-711. PTX-sensitive control responses in this experiment were statistically indistinguishable from the control responses in the prior blinded design, so the control data have been pooled in Fig. 8.

Data analysis and statistics. Unless otherwise noted, error bars represent SE and significance was tested using a one-tailed Student's *t*-test. The choice of a one-tailed as opposed to a two-tailed test was justified because we had an a priori expectation of the direction of the effect. In cases where distributions failed tests of normality by the Shapiro-Wilk test, the Mann-Whitney rank sum (MWRS) test was used as indicated. Data analysis was carried out with Excel, SigmaPlot, and routines written in Matlab R2008.

In all experiments involving photolysis, we defined excitation as the maximum value reached in the 6-s window from the start of the UV flash; this is for all parameters measured, i.e., volley amplitude, latency, and velocity. Inhibition was defined as the minimum value reached in the 11-s window from the start of the UV flash, since the inhibition occurs on a longer time scale than the excitation (Stell 2011). By using this definition, a value for inhibition can be obtained for every experiment, because it is simply the minimum value. This is to be distinguished from the inhibition described in Fig. 3, *A* and *B*, where there was no excitation measured. In the GABA uptake blockade experiments (see Fig. 5), cumulative value differences were calculated by summing the normalized values in the 11-s time window from the start of the UV pulse.

In the experiments involving stimulus intensity variation (see Fig. 4), responses were extremely variable at the lowest stimulus intensities (<10% maximum) with coefficients of variation in baseline amplitude and response that were 80–320% larger than at higher intensities. For this reason we chose to display data from the range of 10% to 100% of normalized baseline amplitude.

In the stimulus train experiments, traces were averaged from four trials per experiment, normalized to the first pulse amplitude, and peak values from each pulse in PTX conditions were subtracted from peak values in control, NNC-711, and cadmium conditions. Because of the temporally correlated nature of these subtracted time series, we chose to test the significance of the cumulative amplitude differences as a time series in each condition. In this case, statistical tests are conducted at successive time points that reflect cumulative differences from the beginning of the train.

NEURON modeling. The compartmental model of the granule cell was constructed in NEURON using mammalian Hodgkin-Huxley channels (Wang et al. 2003). The soma has a diameter of 5.8 μm and

an area of 105.68 μm^2, with resistivity of 1,000 Ω/cm^2, capacitance of 1 $\mu F/cm^2$, sodium channel conductance of 45 mS/cm^2, potassium channel conductance of 18 mS/cm^2, and leak conductance of 30 $\mu S/cm^2$. The axon has the same conductive properties but is 0.3 μm in diameter, with each compartment a single segment 2.5 μm in length. The ascending branch of the fiber is 70 μm in length and branches into two segments of 750 and 250 μm, respectively. For all compartments, the reversal potentials are $V_{Na} = 50$ mV, $V_K = -77$ mV, and $V_L = -70$ mV. Temperature is set at 30°C as in Wang et al. (2003) and Diwakar et al. (2009); however, additional experiments (not shown) conducted at room and physiological temperatures both showed spike facilitation and velocity increases of 108.33% (24°C) and 111.00% (37°C), respectively. In addition to the standard leak conductance and voltage-gated sodium and potassium conductances, we introduced a tonic chloride conductance (G_{GABA}) used to model $GABA_A$Rs. At the soma, this conductance is constant at 100 $\mu S/cm^2$, with a reversal potential (E_{rev}) of −70 mV. Given a 5.8-μm-diameter cell body, this corresponds to a conductance of 423 pS, within the range reported for tonic current in granule cells (Brickley et al. 2001). In the axons, the conductance is $GABA_A$R gated; i.e., it is zero in control and 100 $\mu S/cm^2$ when active, with E_{rev} varying from −75 to −60 mV.

Spike threshold in our model ranges between −48 and −50 mV, considerably more depolarized than any of the E_{Cl} values used in the simulations. To understand the relative contributions of shunting and depolarization on the reported effects, we ran simulations in which we varied the magnitude of G_{GABA} with E_{rev} set at −60 mV. Threshold currents injected at the soma were determined as an indication of excitability. Minimal thresholds were found to occur with G_{GABA} approximately equal to 100 $\mu S/cm^2$. Threshold remained lower than control (i.e., $G_{GABA} = 0$) until G_{GABA} exceeded 1,800 $\mu S/cm^2$, at which point the shunting effect of the conductance predominated over the depolarizing effect and G_{GABA} caused net inhibition. Output from NEURON was analyzed in Matlab R2008.

RESULTS

Compound APs in PFs are enhanced by photolysis of caged GABA. To test whether PF excitability was directly enhanced by $GABA_A$ receptor activation, we performed extracellular recordings of stimulus-evoked population spike activity (fiber volleys) in the molecular layer of acute cerebellar cortical slices cut in a transverse/coronal plane (Fig. 1*A*). An extracellular stimulating electrode and a recording electrode were placed at distances of 80 to 500 μm apart, and fiber volleys were elicited by single stimulus pulses at a frequency of 1 Hz. The external solution contained 100 μM CGP-35348 to block $GABA_B$ receptors and 100 μM CNB-caged GABA. Photolysis of caged GABA transiently enhanced the amplitude (Fig. 1, *B* and C), and this amplitude increase was blocked by either 50 μM SR-95531 or 100 μM PTX ($n = 95$ for control, $n = 68$ for antagonists, $P < 0.001$, MWRS test, Fig. 1*C*), confirming that this resulted from the action of GABA at $GABA_A$Rs. UV excitation in the absence of CNB-GABA had no significant effects on the volley amplitude (101.9 ± 0.6% peak amplitude in UV, 99.0 ± 0.6% minimum amplitude in UV; $P > 0.26$, paired 2-tailed test for the average, minimum, and maximum values reached during the 6 s after the UV vs. the 6 s before the UV, $n = 9$ measurements from 6 slices).

AP conduction velocity is increased by photolysis of caged GABA. We also noticed that the GABA photolysis decreased the latency of the evoked fiber volley and that this effect was sensitive to $GABA_A$R antagonists (control, 136 ± 7 μs advancement relative to pre-UV period; antagonists, 49 ± 6 μs advancement, $n = 95$ and 68, respectively, $P < 0.001$, MWRS test). In the absence of CNB-GABA in the bath solution, UV excitation alone slightly decreased the volley latency (24 ± 7 μs advancement, $n = 9$ measurements from 6 slices), similar to the photolysis responses in $GABA_A$ antagonists ($P = 0.12$, 2-tailed *t*-test).

These decreases in volley latency suggested to us that GABA increased fiber volley conduction velocity. To get a more accurate measurement of conduction velocity, two recording electrodes and a stimulating electrode were positioned in the molecular layer along a beam of PFs so that fiber volley propagation could be recorded (Fig. 1*D*). Conduction velocity was then estimated by

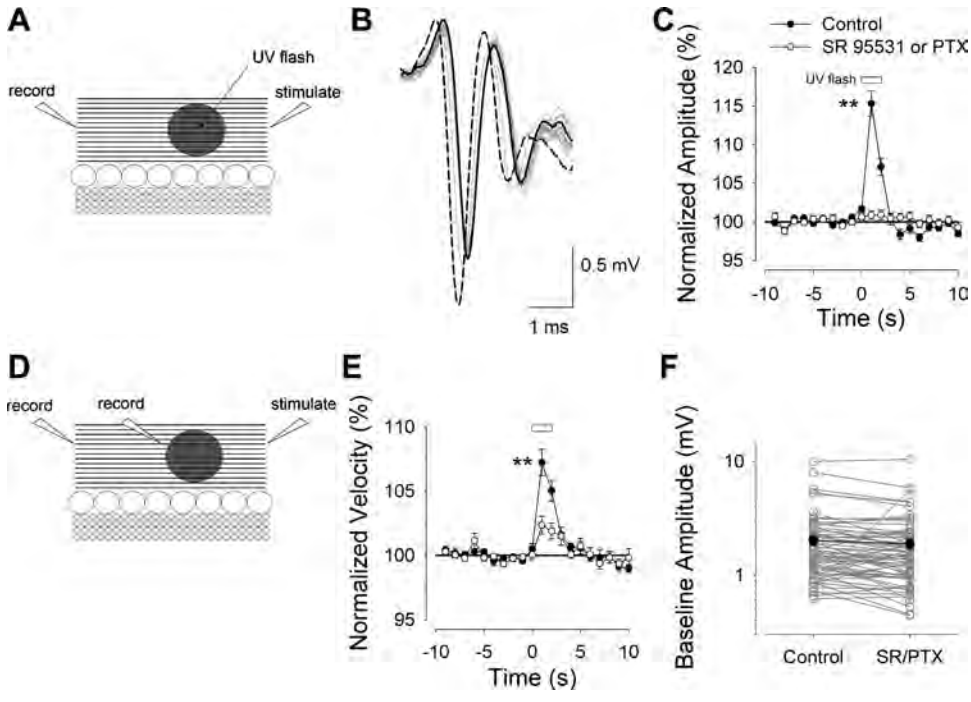

Fig. 1. Local photolysis of GABA excites parallel fibers (PFs) and speeds up fiber volleys. *A*: diagram of the setup of experiments involving 1 recording and 1 stimulating electrode. *B*: sample traces from a single trial. The solid and dashed black traces are, respectively, the volleys recorded immediately at the beginning and 1 s into the UV flash. The gray traces are the volleys recorded at all other times during the experimental protocol. *C*: summary time course ($n = 95$ measurements, 70 slices from 60 animals) from experiments as recorded in *B* and after blockade of $GABA_A$ receptors (GABAARs) by SR-95531 (SR; $n = 28$) or picrotoxin (PTX; $n = 40$). The plot is of the volley amplitude normalized to the average of the 9-s control period before the UV flash. *D*: diagram of the setup of experiments to measure conduction velocity. *E*: summary time course from the velocity experiments in control ($n = 16$ slices, 14 animals) and after wash-in of SR ($n = 3$) or PTX ($n = 10$). *F*: summary of the pre-UV raw volley amplitudes (gray circles) before and after $GABA_A$R blockade by SR or PTX. Average data are denoted by black diamonds. Ordinate axis is log-scaled. In *C* and *E*, a statistically significant difference (**$P < 0.002$) between control and the $GABA_A$R antagonist condition is indicated.

dividing the spatial separation of electrodes by the temporal difference in volley onset. The average conduction velocity we measured in this manner is 0.231 ± 0.046 m/s ($n = 16$), similar to that reported previously (Vranesic et al. 1994). Photolysis of caged GABA increased conduction velocity, an effect sensitive to $GABA_AR$ antagonists (control, 107 ± 1.0%, $n = 16$; $GABA_AR$ antagonists, 103 ± 0.8%, $n = 13$ antagonists, $P = 0.002$, unpaired *t*-test, Fig. 1*E*).

Tonic GABA levels in cerebellar slices activate extrasynaptic forms of $GABA_ARs$ (Santhakumar et al. 2006). To assess whether ambient GABA levels in slices tonically increase PF axonal excitability, we tested whether $GABA_AR$ antagonists change baseline volley amplitude. No significant effects of $GABA_AR$ antagonists were found ($n = 68$, $P = 0.73$, MWRS test, Fig. 1*F*), suggesting that basal levels of GABA in the vicinity of PFs do not increase axonal excitability, either because they are not high enough to activate $GABA_ARs$ or because a persistent presence of GABA is ineffective (Bright et al. 2011).

In these experiments GABA was deliberately photolysed in a large volume to influence as large a population of PFs as possible; this approach has the potentially complicating consequence that $GABA_ARs$ on granule cell bodies may be activated. To test whether the effects of GABA photolysis on fiber volleys are influenced by somatic $GABA_A$ receptors, we carried out a series of experiments in which we surgically removed the granule cell layer, completely severing the connections between granule cell bodies and PF axons (Fig. 2, *A* and *B*). Figure 2, *C* and *D*, summarizes the excitatory actions of GABA photolysis on fiber volley amplitude (127 ± 8.1%, $n = 5$) and latency (advancement of 113 ± 7.9 μs, $n = 5$) in this reduced slice. $GABA_AR$ antagonists significantly inhibited these effects ($P = 0.024$ for amplitude and $P = 5.2 \times 10^{-4}$ for latency). Statistical comparison of these data with the main data set plotted in Fig. 1 indicated that they are not significantly different ($P = 0.11$ for amplitude and $P = 0.47$ for latency, 2-tailed *t*-tests).

A slow inhibitory phase was observed in some slices. There have been reports in several brain regions, including in cerebellar PFs, of axonal $GABA_ARs$ mediating inhibition (Glickfeld et al. 2009; Ruiz et al. 2003; Stell 2011; Zhang and Jackson 1995). When data from all slices were examined, there was evidence of a biphasic effect that manifested as a slight depression in the fiber volley amplitude following the initial peak enhancement. The average minimum reached for all measurements was 95 ± 0.5% ($n = 95$), a significant reduction from the pre-UV pulse baseline ($P = 0.042$, MWRS test). Although significant, because peak depression occurs with a variable latency in different slices, it is barely discernible in the average time course in Fig. 1*C*.

In a minority of slices (6 of 70) we observed monotonic decreases in the volley amplitude with photolysis, and this inhibition was reduced by $GABA_AR$ antagonists (control, 86 ± 2.0%; antagonists, 92 ± 1.3%, $n = 8$ measurements, $P = 0.026$, paired *t*-test; see MATERIALS AND METHODS for how this was calculated; Fig. 3*A*). However, inhibition of fiber volley amplitude in this subset of experiments was not accompanied by delays of the volley arrival or decreases in fiber volley velocity. In fact, it was associated with significantly increased conduction velocity (latency: 161 ± 31 μs, $n = 11$ measurements in 8 slices; velocity: 107 ± 1%, $n = 3$ slices, $P < 0.02$, paired *t*-tests). This "pure" inhibition decreased in older animals (Fig. 3*B*), a developmental profile distinct from that exhibited by excitation (Fig. 3*C*).

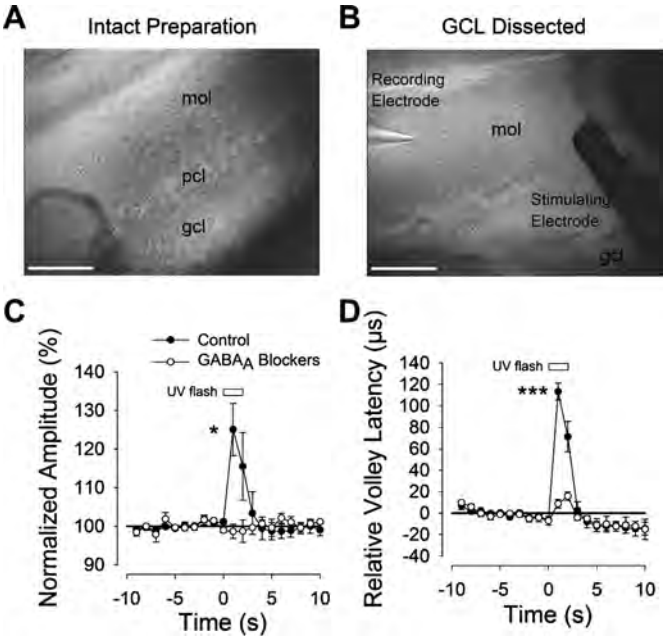

Fig. 2. GABA excitation of PF axons is not due to GABA actions at the granule cell bodies. *A*: photograph of an intact slice preparation. gcl, Granule cell layer; pcl, Purkinje cell layer; mol, molecular layer. Scale bars (in A and *B*), 100 μm. *B*: photograph of a slice preparation with the stimulating electrode and recording electrode in view. The granule cell layer was dissected away from the molecular layer by making an incision between the granule cell layer and the molecular layer with a 27-gauge syringe needle under ×30 magnification. *C*: summary time course of the normalized volley amplitude ($n = 5$ measurements, 4 slices from 4 animals) from experiments as carried out in Fig. 1*B* and after blockade of $GABA_ARs$ by SR or PTX. *D*: summary time course of the volley latency after subtraction of the average latency in the pre-UV period from the same experiments as in *C*. In *C* and *D*, significant differences (*$P = 0.024$; ***$P = 0.00052$) between control and $GABA_AR$ antagonist conditions are indicated. Neither amplitude ($P = 0.11$) nor latency ($P = 0.47$) in the dissected slice are significantly different from the group data obtained in intact slices in Fig. 1.

$GABA_BR$ receptors on PF axon terminals inhibit calcium influx but have been reported to modestly inhibit PF volley amplitudes recorded with voltage-sensitive dyes (Dittman and Regehr 1997; Sabatini and Regehr 1997). All experiments presented to this point included the $GABA_BR$ receptor antagonist CGP-35348. To test whether $GABA_BR$ receptors influence the fiber volley and conduction velocity or may contribute to the slow inhibitory effects, we compared photolysis responses before and after addition of the $GABA_BR$ receptor antagonist CGP-35348. We observed similar excitatory actions of GABA photolysis on fiber volley amplitude and latency in the absence of CGP-35348 and no significant change after addition of the antagonist (normalized volley amplitude: control, 123 ± 2.8%; CGP-35348, 126 ± 3.8%, $P = 0.11$, paired *t*-test; relative volley latency: control, 84 ± 14.6 μs; CGP- 35348, 89 ± 13.5 μs, $P = 0.18$, paired *t*-test, $n = 5$). Inhibitory actions were also unaffected (control, 92 ± 2.5%; CGP-35348, 91 ± 2.9%, $P = 0.58$, paired 2-tailed *t*-test). Together these results show that the inhibitory effects are relatively small and slow compared with the excitatory effects and are dependent on $GABA_ARs$ but unrelated to $GABA_BR$ receptors.

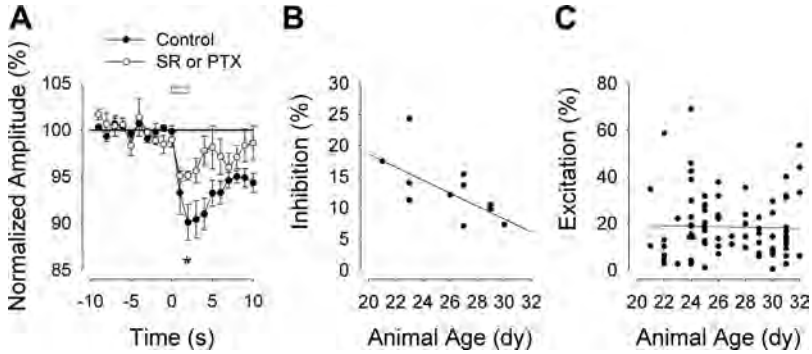

Fig. 3. Summary of excitatory and inhibitory effects of GABA on volley amplitude. *A*: summary time course from experiments as carried out in Fig. 1*B*, but only from those experiments which showed an inhibitory effect on volley amplitude. Here, inhibition is defined as no increase in volley amplitude by UV and a decrease in volley amplitude to <95% of baseline average in the first 5 s after the UV pulse (control, $n = 11$ measurements, 8 slices from 8 animals; SR, $n = 3$; PTX, $n = 3$). *B*: scatter plot of the volley amplitude inhibition by UV vs. the age of the animal from the same experiments reported in *A* (parameters of the linear fit: $y = 41.24 - 1.09x$, $R^2 = 0.435$). *C*: scatter plot of the volley amplitude enhancement by UV vs. the age of the animal (linear fit: $y = 22.3 - 0.14x$, $R^2 = 0.0013$). Note that all experiments in Fig. 1*C* are displayed as individual points in either *C* or *B*. The triangle in C corresponds to the representative trace shown in Fig. 1*B*. In *A*, a significant difference (*$P = 0.026$) between control and the SR/PTX condition is indicated.

Recruitment of more axons accounts for the increase in fiber volley amplitude. To further explore the mechanism underlying GABA-mediated excitation of PFs, we carried out experiments similar to those described above but using a range of electrical stimulus intensities. If the excitatory effect of GABA increases the probability of eliciting a spike in individual axons, then as the electrical stimulus intensity is raised, the increase of volley amplitude evoked by GABA photolysis should be smaller, since there will be progressively smaller pools of axons to recruit. We found a robust, inverse correlation between percent enhancement and baseline fiber volley amplitude (Fig. 4*A*), consistent with the view that GABA is increasing the probability that an axon is brought to threshold at a given stimulus intensity. No correlation was observed for inhibition vs. baseline volley amplitude (Fig. 4*B*). We also tested whether the magnitude of the conduction volley increase varied with stimulus intensity and found no correlation consistent with a mechanism that does not depend on fiber recruitment (Fig. 4*C*).

The magnitude of the photolysis effect was dependent on the clearance rate of GABA from the extracellular space surrounding the axons. Blockade of the GABA transporter GAT-1 by NNC-711 (10 μM) significantly increased the peak enhancement of volley amplitude by photolysis and prolonged the time course of the photolysis increase ($n = 14$, $P = 0.0007$, paired 2-tailed test comparing cumulative amplitudes of control vs. drug, Fig. 5, *A* and *B*). NNC-711 did not significantly increase the peak enhancement of velocity, but it did prolong the time course of velocity increase, although this effect did not reach significance ($n = 5$, $P = 0.059$, paired 2-tailed test, Fig. 5, *C* and *D*). Two other GABA transporter isoforms, GAT-2 and GAT-3, are not expressed in the cerebellar cortex (Clark et al. 1992; Durkin et al. 1995). Consistent with this, the GAT-2- and GAT-3-specific antagonist SNAP-5114 had no significant effect on the photolysis enhancement of volley amplitude (cumulative amplitude change: control, 79 ± 18%, SNAP-5114, 54 ± 16%, $P = 0.15$, paired 2-tailed test; $n = 9$ measurements in 5 slices from 4 animals).

Subunit requirement of axonal $GABA_A$Rs mediating excitation. To obtain insight into the molecular composition of the axonal $GABA_A$Rs mediating this excitatory effect, we tested a series of drugs that target different $GABA_A$R subtypes. We first tested etomidate, a widely used intravenous anesthetic that enhances currents from all $GABA_A$Rs containing either a β_2- or β_3-receptor, independent of whether γ- or δ-subunits are present (Belelli et al. 1997; Meera et al. 2009). Etomidate (5 μM) increased the excitatory effect of GABA photolysis on volley amplitude ($P = 0.038$, paired *t*-test, $n = 8$, Fig. 6, *A* and *B*). In addition, etomidate enhanced the inhibition that followed the initial excitation (Fig. 6*A*, $P = 0.006$, paired *t*-test).

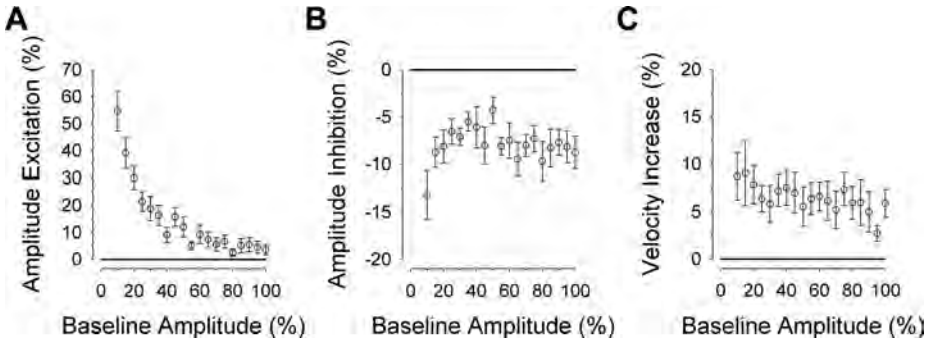

Fig. 4. Relationship of GABA photolysis effects with stimulus intensities. *A*: plot of normalized amplitude excitation by GABA vs. normalized baseline volley amplitude. Experiments were carried out as in Fig. 1, but the stimulus duration was varied systematically between trials. All volley amplitude values for a single experiment were normalized to the peak volley amplitude for the entire experiment, and then the data were binned (5% bin width) and averaged ($n = 17$ measurements, 9 slices from 9 animals). *B*: plot of normalized amplitude inhibition vs. baseline volley amplitude (from the same experiments as in *A*; see MATERIALS AND METHODS for discussion of how inhibition was defined). *C*: plot of normalized velocity increase vs. baseline volley amplitude ($n = 8$ slices from 8 animals).

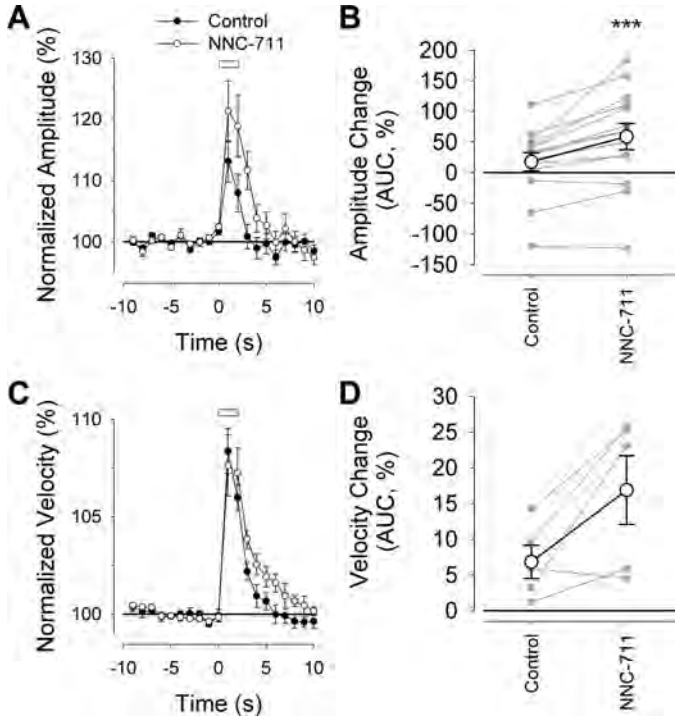

Fig. 5. Blockade of GABA reuptake prolongs the photolysis effect: NNC-711 summary data. *A*: time course of volley amplitude ($n = 14$ measurements, 9 slices from 7 animals). *B*: cumulative amplitude change (AUC) are summarized (individual data in gray circles, group average and SE in open diamonds, see MATERIALS AND METHODS for discussion of how these values were calculated). The solid black lines here and in *D* indicate the expected AUC values if there had been no changes from the baseline; therefore, values above and below the solid black line represent net excitation and inhibition, respectively. A significant difference (***$P = 0.0007$) between control and NNC-711 conditions is indicated. *C*: time course of volley velocity ($n = 5$ slices from 4 animals). *D*: velocity AUC summary data as described in *B*.

We then tested the more specific allosteric modulator diazepam, a benzodiazepine that enhances currents from $GABA_A$Rs that both lack the α_4- and α_6-subunits and contain a γ-subunit (Mohler et al. 2001). Diazepam (1 μM) had no significant effects on either the excitatory or inhibitory actions of GABA photolysis on volley amplitude (excitation: $P = 0.65$, MWRS test, $n = 9$; inhibition: $P = 0.39$, paired *t*-test, Fig. 6, *C* and *D*). As discussed in MATERIALS AND METHODS, photolysis-induced GABA concentration transients within the slice are unlikely to saturate $\alpha_1\beta_{2/3}\gamma_2$ receptors, the only receptor subtypes present on PFs that would be diazepam sensitive (Santhakumar et al. 2006). Thus we interpret the lack of diazepam sensitivity to rule out $\alpha_1\beta_{2/3}\gamma_2$ receptor subtypes as major contributors to the potentiating effect of GABA on PF axons.

The $GABA_A$R δ-subunit has been shown to be extrasynaptically localized in the cerebellum, hippocampus, and other brain regions (Brickley et al. 1996; Farrant and Nusser 2005). Also, δ-containing $GABA_A$Rs are reported to be expressed at mossy fiber terminals in the hippocampal dentate gyrus, where they mediate a depolarizing action of GABA (Ruiz et al. 2010). To determine whether the excitatory GABA effects on PFs require the δ-subunit, we first tested the drug DS2, which has been shown to be a specific positive allosteric modulator of $GABA_A$Rs containing the δ-subunit (Shu et al. 2011; Wafford et al. 2009). There were no significant effects of DS2 (10 μM) on the excitatory phase of volley amplitude ($n = 8$, $P = 0.11$, paired *t*-test, Fig. 7, *A* and *B*); however, DS2 enhanced the inhibitory phase ($P = 0.03$, paired *t*-test, Fig. 7*A*).

We then carried out the same photolysis experiments in cerebellar slices from mice lacking the δ-subunit gene. These mice lack tonic $GABA_A$R-mediated currents in the cell bodies (i.e., granule cells) of PF axons (Meera et al. 2011; Stell et al. 2003). Photolysis of GABA in slices from $GABA_A$R antagonists significantly inhibited the response in $\delta^{-/-}$ slices ($n = 10$, $P = 0.032$, MWRS test, Fig. 7*C*). Photolysis of GABA in slices from $\delta^{-/-}$ mice was statistically indistinguishable from that observed in slices from wild-type mice ($n = 12$ for $\delta^{-/-}$ group, $P = 0.25$, MWRS test, Fig. 7*C*), indicating that the δ-subunit is not required for this excitatory action of GABA.

Endogenously released GABA can excite PFs. To determine whether endogenous GABA released by molecular layer interneurons can also excite PFs, we carried out experiments in which stimulus trains (20 Hz) were delivered to the molecular layer while fiber volleys were recorded 300–500 μm away in the presence of a $GABA_B$R blocker (Fig. 8*A*). As compound APs, fiber volley amplitudes varied during trains, typically increasing in amplitude steeply during the first 0.4 s and reaching a steady-state amplitude ~1 s into the train (Fig. 8*B*). To isolate the $GABA_A$R-dependent effects, we compared trains in the absence and presence of the $GABA_A$R antagonist PTX and calculated the $GABA_A$R-dependent change in fiber volley amplitude during the train normalized to the amplitude of the first pulse (Fig. 8*C*). To assess whether $GABA_A$R-dependent increases in fiber volley amplitude are due to GABA

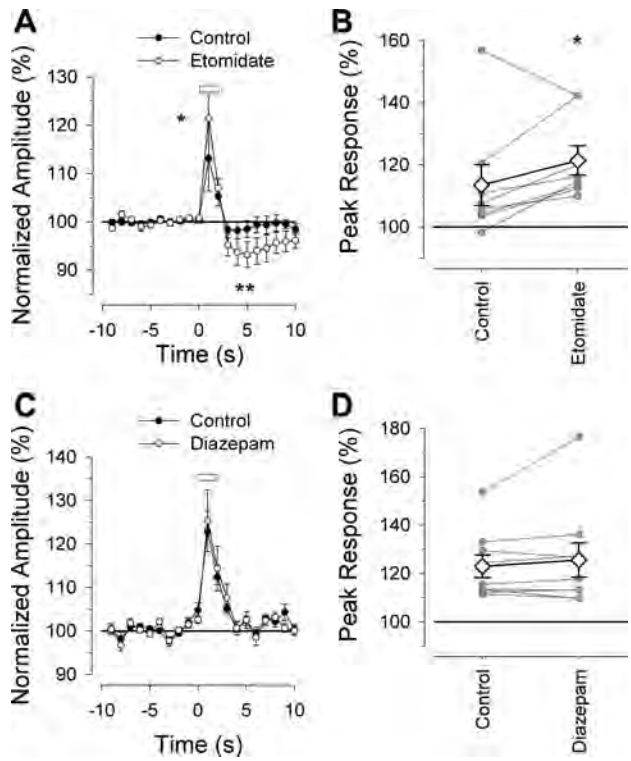

Fig. 6. Axonal $GABA_A$Rs mediating photolysis effect are sensitive to etomidate but not to classical benzodiazepines. *A* and *B*: etomidate summary data. *A*: time course of volley amplitude ($n = 7$ measurements, 7 slices, 7 animals). *B*: amplitude summary data. Significant differences (*$P = 0.038$; **$P = 0.006$) between control and etomidate conditions are indicated. *C* and *D*: diazepam summary data. *C*: time course of volley amplitude ($n = 8$ measurements, 5 slices from 5 animals). *D*: amplitude summary data.

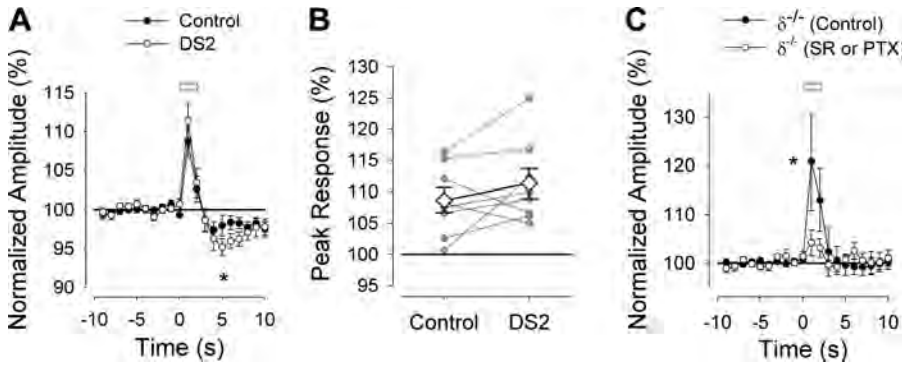

Fig. 7. Excitation of PFs by GABA does not require the $GABA_AR$ δ-subunit. *A* and *B*: DS2 summary data. *A*: time course of volley amplitude ($n = 8$ measurements, 8 slices, 8 animals). Comparisons between control and DS2 were not significantly different for the excitatory phase ($P = 0.11$) but were for the inhibitory phase ($P = 0.03$). *B*: amplitude summary data. *C*: time course of volley amplitude in $\delta^{-/-}$ mice (control, $n = 12$ slices, 10 animals; SR, $n = 3$; PTX, $n = 7$). A significant difference ($^*P = 0.032$) between control and $GABA_AR$ antagonist conditions is indicated.

released from interneurons, we used a blinded experimental design to compare responses in control solution with responses in solution containing the calcium channel blocker cadmium (100 μM). After the initial 0.4-s transient rising phase, there was a significant PTX-sensitive response in the control condition but not in the cadmium condition (control, $n = 6$, $0.027 < P < 0.050$; cadmium, $n = 6$, $0.17 < P < 0.490$, Fig. 8*C*). These results demonstrate that synaptic transmission is re-

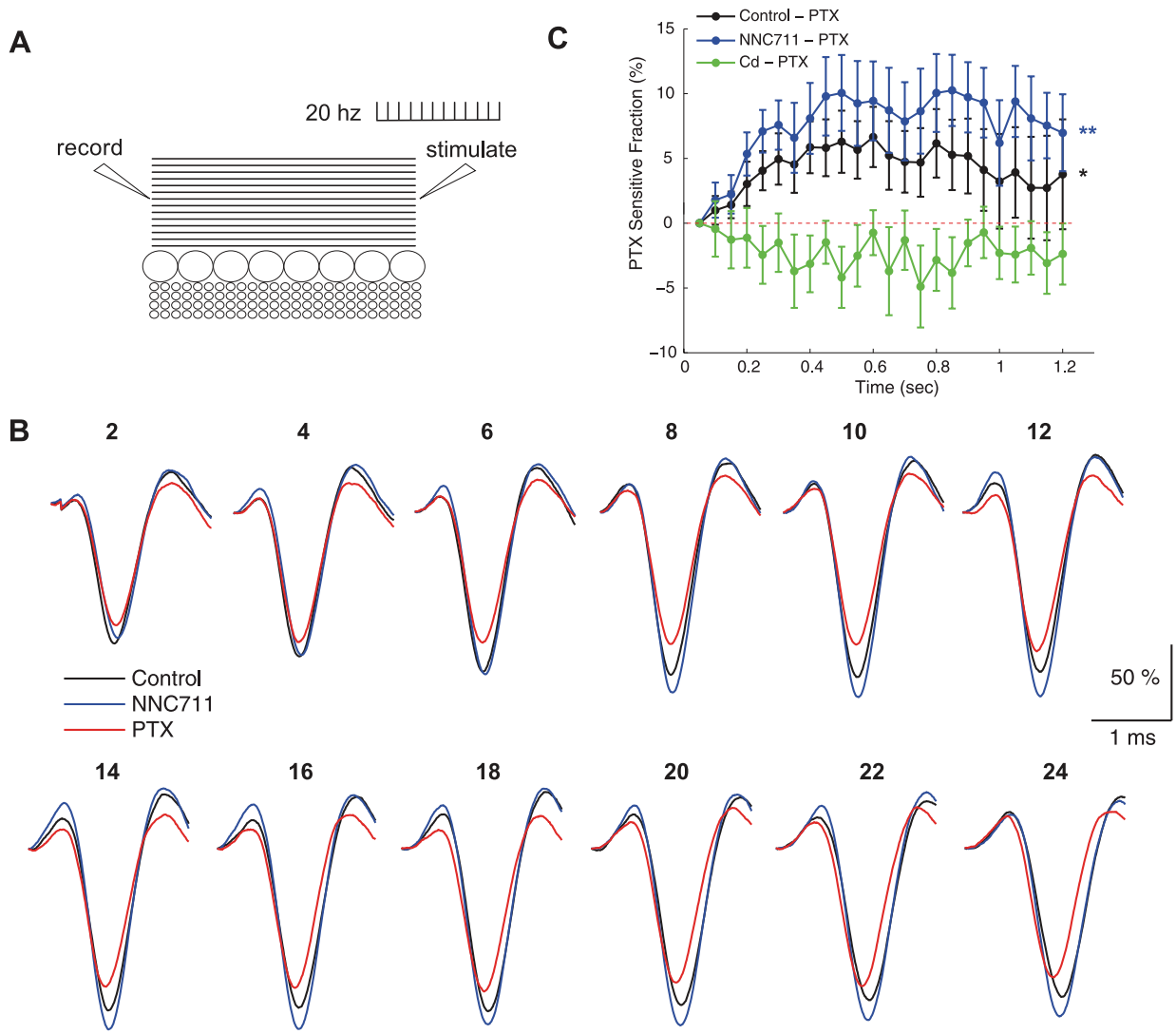

Fig. 8. Endogenously released GABA contributes to PF excitation. *A*: diagram of the experimental design. *B*: sample fiber volleys in response to 20-Hz stimulation. Traces have been normalized to the amplitude of the first fiber volley in the train, and numbers above traces indicate the pulse number in the train. Black traces are control, blue traces are in the GABA uptake blocker 10 μM NNC-711, and red traces are in 10 μM NNC-711 and 100 μM PTX. *C*: mean time courses of the PTX-sensitive components in control (black, $n = 16$), 100 μM Cd (green, $n = 6$), and 10 μM NNC-711 (blue, $n = 10$). PTX-sensitive components are expressed as a fraction of the amplitude of the first fiber volley in the train. Control data for cadmium and NNC-711 experiments are pooled in this plot (see RESULTS). Significant differences from no change were found for cumulative, PTX-sensitive components in control ($^*P = 0.042$) and NNC-711 ($^{**}P = 0.004$). Control and NNC-711 components are significantly different from one another in the time period from 0.8 to 1.2 s ($P < 0.05$).

quired for the $GABA_AR$-dependent effect and imply that fiber volley amplitudes are altered by the release of GABA from molecular layer interneurons.

We next examined whether the GABA uptake blocker NNC-711 further enhanced this effect. Analysis of the cumulative PTX-sensitive change in the time period from 0 to 0.75 s showed significant increases in the control condition; because this control was indistinguishable from the control condition above (Kolmogorov-Smirnov 2-sample test, $0.08 < P < 0.82$ for time points between 0 and 1.2 s), control data have been pooled in Fig. 8*C*. For both control and NNC-711 conditions, PTX-sensitive responses cumulated over the time period from 0 to 0.75 s were significantly enhanced from no change (Fig. 8*C*, control in black, $n = 10$, $P = 0.042$; NNC-711 in blue, $n = 10$, $P = 0.004$). Although there was a trend toward larger increases throughout the train in the presence of the GABA reuptake inhibitor, the difference between control and NNC-711 only became significant late in the train (0.8–1.2 s, $n = 10$, $0.034 < P < 0.05$). Together these data suggest that GABA release from molecular layer interneurons can excite PF axons and facilitate the amplitude of fiber volleys during trains.

Depolarizing $GABA_AR$ actions in a compartmental model of granule cell and PF axon. To establish whether a regional difference in chloride concentration in axonal compartments could account for increased axonal excitability in PFs, we implemented a NEURON model of a granule cell body and bifurcating PF axon with mammalian Hodgkin-Huxley-style conductances (Wang et al. 2003). The model consists of a 5.8-μm-diameter cell with a 0.3-μm-diameter axon (Fig. 9*A*). The axon ascends for 70 μm and then bifurcates into two branches, one 750 μm and the other 250 μm. Each axonal compartment is 2.5 μm in length. All compartments have a constant density of leak conductance, voltage-gated potassium conductance, and voltage-gated sodium conductance. To mimic tonic inhibition, all simulations include a constant conductance of 100 $\mu S/cm^2$ ($E_{rev} = -70$ mV) at the cell body in addition to the standard leak conductance.

To simulate GABA effects on the axon, gated GABA conductances with user-defined reversal potentials designated as $G_{GABA,\ Erev}$ are added selectively to axonal compartments. In this way the model can be used to explore how PF axon excitability is affected by regional activation of axonal con-

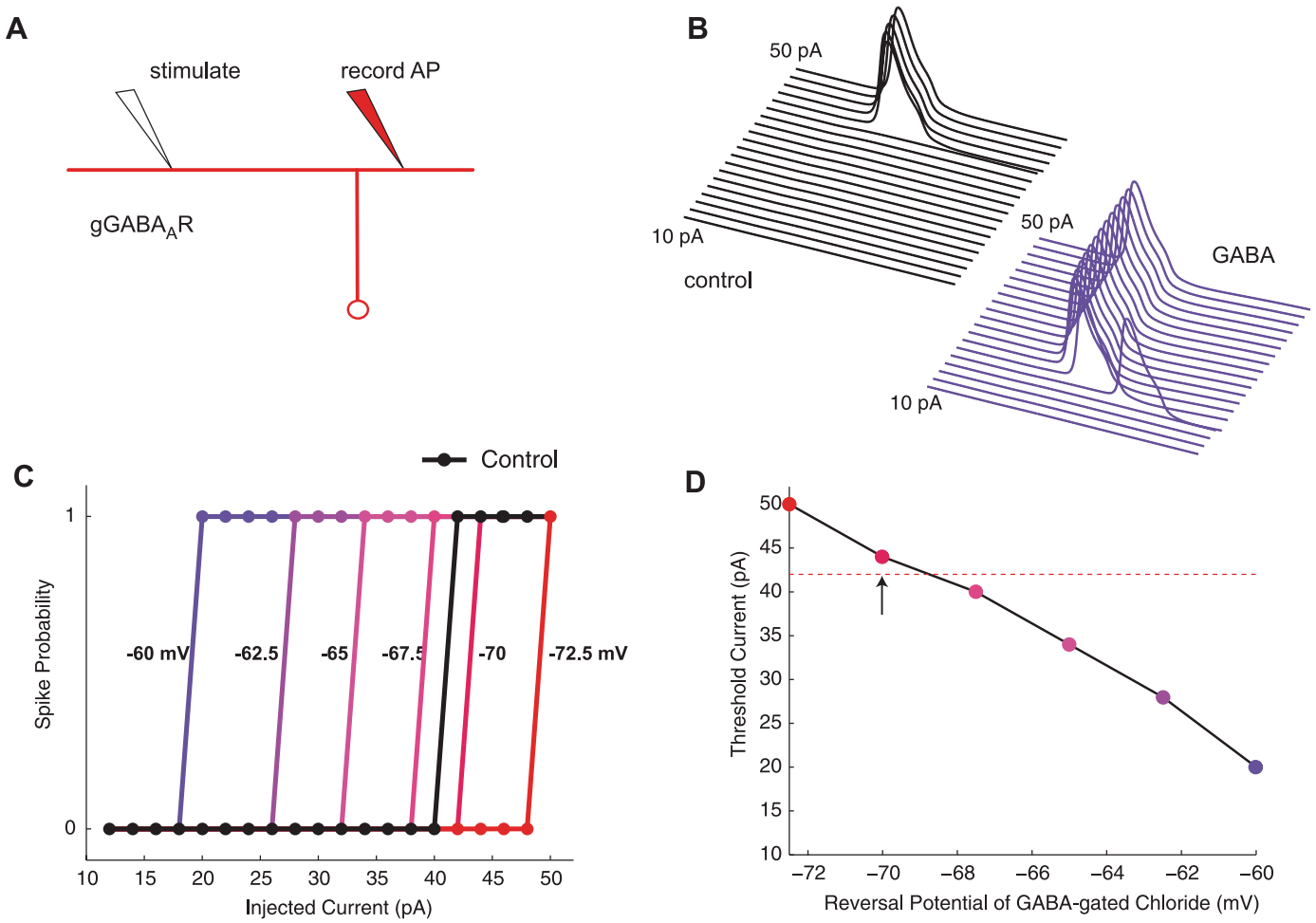

Fig. 9. Simulation of the effect of $GABA_AR$-activation on axonal excitability. *A*: diagram of the NEURON simulation. *B*: a family of responses recorded in the axon in response to an ascending range of current injections (1-ms duration, 10–50 pA) into a site in the axon 600 μm away. Black traces indicate control, and purple traces indicate conditions in which an axonal GABA conductance (G_{GABA}; 100 $\mu S/cm^2$, −60 mV reversal potential for chloride) is active. Trace durations are 25 ms. *C*: spiking probability as a function of stimulus size. Each color shows the effect of a GABA-gated chloride conductance (100 $\mu S/cm^2$) with a different reversal potential. *D*: threshold current as a function of G_{GABA} reversal potential. Horizontal line shows the threshold current for control condition ($G_{GABA} = 0$). Arrow indicates the resting potential of −70 mV; note that activation of $G_{GABA,\ -70\ mV}$ leads to an increase in threshold.

ductances with a range of reversal potentials from −55 to −75 mV, that is, $G_{GABA,\ -55\ mV}$ to $G_{GABA,\ -75\ mV}$.

When $GABA_AR$ conductances (100 $\mu S/cm^2$) were activated in the axon, the threshold for spike generation triggered by current injection in the axon was reduced in a manner dependent on the reversal potential. Activation of $G_{GABA,\ -60\ mV}$ in the axon decreased spike threshold to 40% (Fig. 9, *B–D*). In contrast, with $G_{GABA,\ -70\ mV}$, that is, a reversal potential set equal to the resting membrane potential of the axon, spike threshold increased slightly, presumably due to shunting inhibition (Fig. 9, *C* and *D*). Increases in spike threshold were also observed for $G_{GABA,\ -75\ mV}$.

Experiments on single PF axons suggest that axonal G_{GABA} might also affect orthodromic spike initiation (Pugh and Jahr 2011). To test whether the model shows this behavior, currents were injected into the granule cell body to elicit spikes (Fig. 10*A*). Activation of axonal G_{GABA} also decreased orthodromic spike threshold in a manner dependent on reversal potential (Fig. 10, *B* and *C*). In this case no shunting was seen for the threshold curve when the reversal potential for G_{GABA} was equal to the resting membrane potential. However, a small delay in time to spike was observed when the reversal potential for G_{GABA} was equal to the resting membrane potential consistent with shunting (Fig. 10*D*, compare control and −70-mV curves). Considered together, the modeling results suggest that axonal G_{GABA} decreases threshold for orthodromic spikes, facilitating normal spike generation.

We next examined whether activation of axonal G_{GABA} affected conduction velocity by depolarizing the cell body and measuring AP propagation at two sites in the axon (Fig. 11*A*). As was the case for the threshold effect, GABA-induced changes in conduction velocity varied with $G_{GABA,\ Erev}$ such that conduction velocity was inhibited by 6.3% $G_{GABA,\ -75\ mV}$ and increased by 10.3% at $G_{GABA,\ -60\ mV}$.

To better understand how axonal depolarization increases conduction velocity we explored changes in the properties of the voltage-gated sodium conductance. Given that G_{GABA} is depolarizing the axon, we reasoned that increases in conduction velocity would be sensitive to the voltage dependence of sodium channel availability, as formalized in the h_∞ curve. To test this hypothesis, we modified the mammalian version of sodium conductance (Wang et al. 2003) used in the earlier simulations so that it would have an h_∞ curve identical to that of the original Hodgkin-Huxley (HH) sodium channel (Hodg-

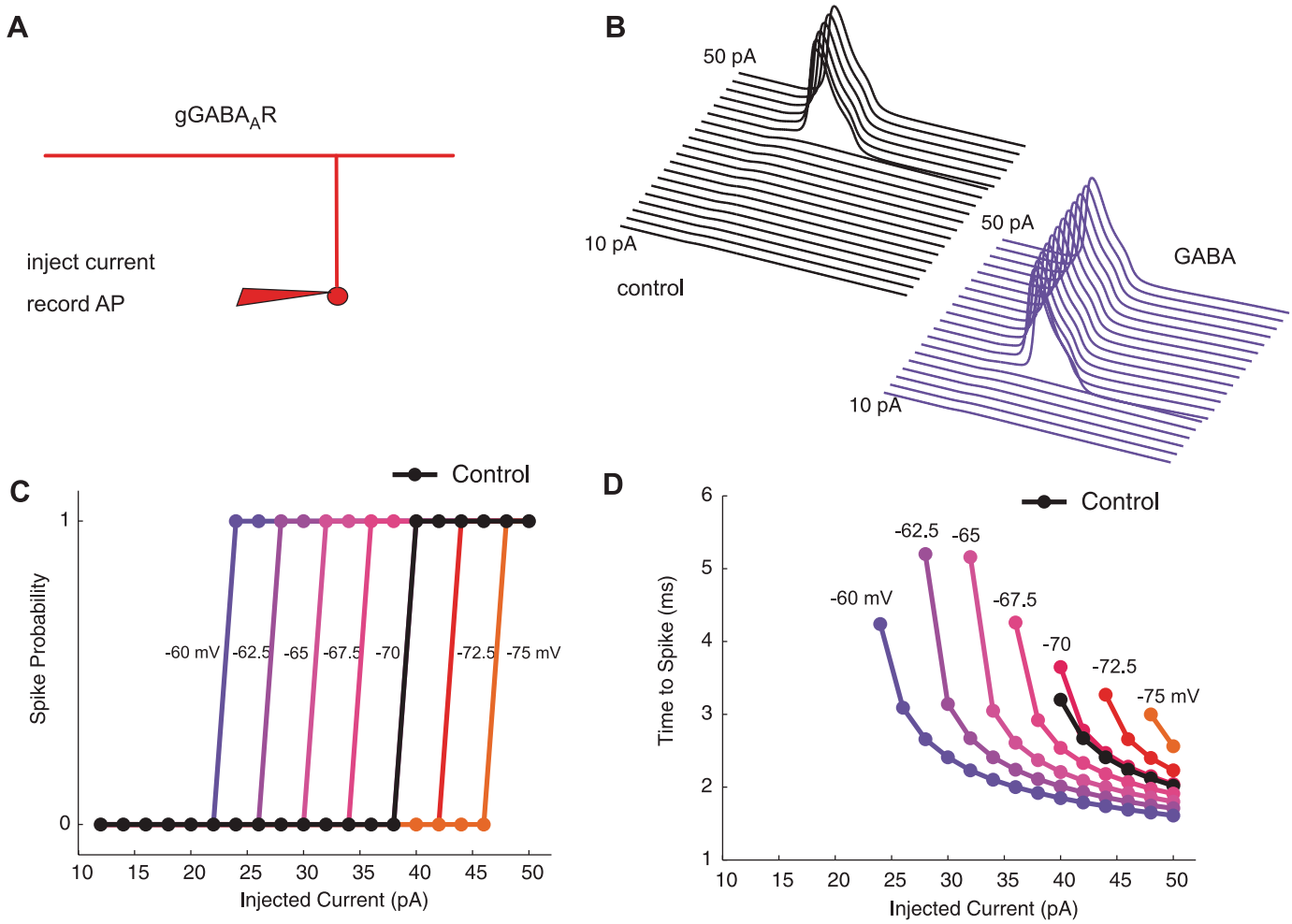

Fig. 10. Simulation of the effect of $GABA_AR$-activation on orthodromic spike initiation. *A*: diagram of the NEURON model. *B*: traces recorded in the soma in response to a range of stimulus intensities. Black traces indicate control (G_{GABA} = 0), and purple traces indicate $G_{GABA,\ -60\ mV}$ = 100 $\mu S/cm^2$. *C*: spiking probability curves in response to current injection at the soma. Different colors indicate reversal potentials for G_{GABA}. *D*: time to spike for action potentials (AP) at the soma vs. stimulus current. Each color represents simulations at different reversal potentials for G_{GABA}. Note the slight shunting effect apparent as a slightly longer delay to spike in comparing $G_{GABA,\ -70\ mV}$ (red) with control (black).

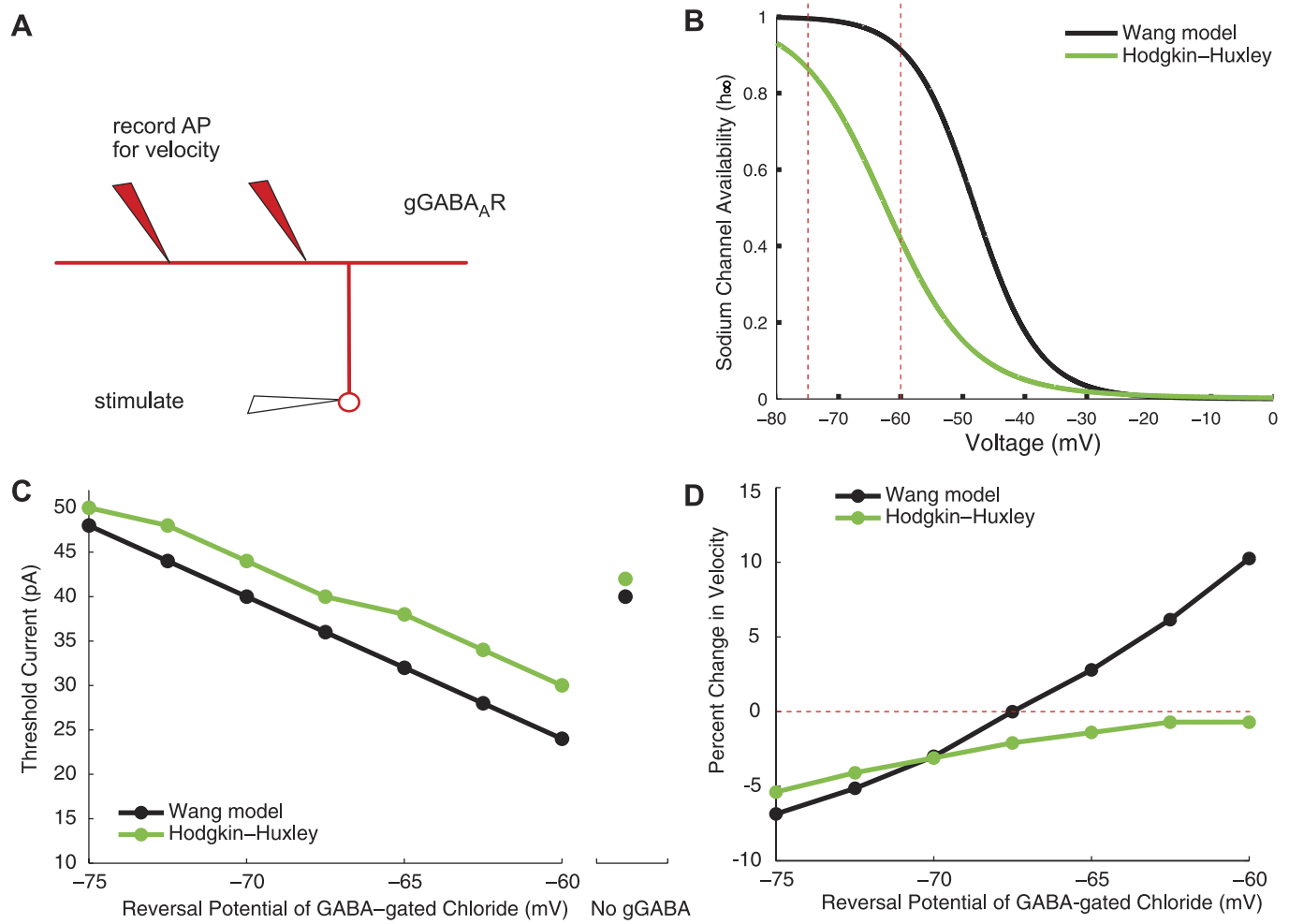

Fig. 11. Sodium channel h∞ curves influence the effect of depolarizing GABA on conduction velocity. *A*: diagram of the NEURON model for studying conduction velocity. The two recording spots are 170 and 570 μm away from the cell body. *B*: sodium channel availability (h∞) curves for the mammalian Hodgkin-Huxley model (Wang 2003) and the squid giant axon Hodgkin-Huxley model (Hodgkin-Huxley 1952). The range of $G_{GABA,\ Erev}$ simulated in this study is indicated by the vertical red lines. *C*: threshold current for generating an AP as a function of G_{GABA} reversal potential. Black curve indicates simulations using the h∞ curve from Wang 2003, and green curve represents simulations using the Hodgkin-Huxley h∞ curve. Symbols at *right* show the threshold current for control conditions ($G_{GABA} = 0$) in the 2 models. *D*: percent change in conduction velocity vs. reversal potential for the 2 models.

kin and Huxley 1952). With an HH channel, fewer than half as many sodium channels are available at −60 mV as are available at −75 mV (Fig. 11*B*, green curve) compared with a loss of only 10% over the same membrane potential range with the mammalian channel (Fig. 11*B*, black curve). In simulations using the HH sodium channel, the resting membrane potential was unchanged (−70 mV in both models with $G_{GABA} = 0$) and G_{GABA} still decreased threshold, albeit to a smaller extent (Fig. 11*C*). However, G_{GABA}-induced increases in conduction velocity were lost; instead, conduction velocity was decreased at all chloride reversal potentials (Fig. 11*D*).

DISCUSSION

We have found that transient activation of GABA$_A$Rs on PFs increases axonal excitability and that this is reflected in an increase in the amplitude of fiber volleys and an increase in axonal conduction velocity. Our findings complement previous studies which have suggested that PF presynaptic excitability is increased by GABA (Pugh and Jahr 2011; Stell 2011; Stell et al. 2007). In the prior work, pressure pipette application of GABA and/or muscimol or iontophoretic application of GABA was found to increase glutamate release from PFs (Pugh and Jahr 2011; Stell et al. 2007) and to increase PF calcium transients (Pugh and Jahr 2011; Stell 2011). Calcium imaging of single PF axons as well as whole cell recording from granule cell bodies demonstrated that GABA application to axons reduces the threshold for generating an AP (Pugh and Jahr 2011). The fiber volley measurements described here extend these observations, demonstrating directly that axonal membrane excitability is altered and that this affects not only presynaptic output but also spike propagation.

The most likely mechanism by which GABA excites PFs is by depolarizing the axonal membrane, thereby bringing the axon closer to AP threshold. In this way the axon could provide passive depolarization to the spike initiation zone, acting in a manner analogous to that of a dendrite. Experimental evidence is consistent with passive propagation of GABA$_A$R-initiated depolarization over considerable distances in PF axons (Pugh and Jahr 2011). Moreover, modeling studies suggest that APs are initiated in the ascending axon of PFs (Diwakar et al. 2009), supporting the idea that axonal GABA$_A$Rs can influence orthodromic spike generation.

It has been hypothesized that the depolarizing effect of GABA on PFs is due to slightly higher chloride concentrations in the axon (Pugh and Jahr 2011; Stell 2011; Stell et al. 2007). PFs would thus be similar to mossy fiber axons, calyx of Held nerve terminals, and pituitary nerve terminals, preparations in which cell-attached and perforated patch-clamp recordings have demonstrated GABA depolarization of the terminal (Price and Trussell 2006; Ruiz et al. 2010; Zhang and Jackson 1995). In the latter two preparations, noninvasive recordings have also allowed estimates of internal chloride concentrations of 15–20 mM and corresponding GABA reversal potentials of approximately −50 mV (Price and Trussell 2006; Zhang and Jackson 1995).

The inaccessibility of PFs to patch-clamp methods has made it impossible to directly explore whether there are regional differences in chloride reversal potential in PFs. However, the pattern of expression of chloride cotransporters in cerebellar granule cells and PF axons suggests that regional differences in chloride reversal potential may exist. Chloride gradients in neurons are determined in large part by the actions of two types of chloride transporters, KCC2, which extrudes chloride, and NKCC1, which accumulates chloride into neurons (Blaesse et al. 2009). In some brain regions, such as the olfactory neuroepithelium, retina, and suprachiasmatic nucleus, where GABA has been shown to be excitatory, NKCC1 protein has been detected in adult tissue (Belenky et al. 2009; Kaneko et al. 2004; Li et al. 2008). In other neurons, such as neocortical pyramidal cells, where GABA has been shown to depolarize axons, it is unclear whether NKCC1 is expressed in adults; however, KCC2 protein is excluded from the axonal compartments (Szabadics et al. 2006). In the adult cerebellar cortex, both KCC2 and NKCC1 mRNA are present in granule cells (Mikawa et al. 2002), and KCC2 protein appears to be completely absent in PFs (Seja et al. 2012). Thus, either the presence of NKCC1 or the absence of KCC2 from PFs likely accounts for the compartmental differences in chloride reversal potential.

The $GABA_AR$ subtype responsible for exciting PFs. Our data in slices are consistent with axonal $GABA_A$Rs being entirely responsible for the increase in excitability (Fig. 2). Indeed, under our experimental conditions, it is unlikely that activation of somatic $GABA_A$Rs could have contributed. The effect of GABA on granule cell bodies is hyperpolarizing; therefore, if there were any contribution to axonal excitability, it would be inhibitory. Moreover, local iontophoresis of GABA onto single PF axons yields a very similar effect to that described here (Pugh and Jahr 2011).

Cerebellar granule cells express a unique isoform of $GABA_A$R containing δ- and α_6-subunits that is localized on extrasynaptic membranes and which knockout studies show is responsible for a tonic GABA current (Brickley et al. 2001; Meera et al. 2011; Nusser et al. 1998; Santhakumar et al. 2006; Stell et al. 2003). We found that DS2, a modulator selective for δ-subunit-containing $GABA_A$Rs (Shu et al. 2011; Wafford et al. 2009), did not affect the enhancement by GABA on volley amplitude or volley latency; however, it did enhance the inhibitory phase that sometimes followed the initial excitation. If the inhibitory phase arises from persistent activation of PF $GABA_A$Rs, as we argue below, then it is likely the case that δ-$GABA_A$Rs are involved in excitation as well as inhibition but that in DS2 the inhibitory effect dominates. Nevertheless, GABA-mediated excitation of PFs was present in tissue from mice lacking the δ-subunit, indicating that although δ-subunits may be present on PFs, they are not required for GABA-mediated excitation of PFs.

Immunocytochemistry suggests that δ protein, like α_6, is expressed highly in granule cell somata and at much lower levels, if at all, in the molecular layer (Pirker et al. 2000). We have demonstrated here that etomidate enhances the excitatory effect of GABA uncaging on PFs but that diazepam has no effect. This pharmacological profile, sensitivity to etomidate but not to classical benzodiazepines, suggests that PF $GABA_A$Rs either lack a γ-subunit or contain α_6, or both (Mohler et al. 2001). Considering that α_1 protein is detected in presynaptic terminals in PF boutons by electron microscopy (Stell et al. 2007) and that α_6-containing $GABA_A$Rs increase PF release of glutamate (Schmid et al. 1999), a reasonable possibility is that $GABA_A$Rs on PFs are composed of α_1, α_6, $\beta_{2/3}$, and γ_2 or δ. Biochemical and electrophysiological data support the presence of such a receptor subtype on somatodendritic membranes of granule cells (Jechlinger et al. 1998; Santhakumar et al. 2006), although it is also possible that receptors composed only of α- and β-subunits are involved as has been suggested in hippocampus (Mortensen and Smart 2006). Together, our data and published literature are consistent with axonal $GABA_A$Rs of the subunit composition $\alpha_{1/6}\beta_{2/3}\delta$, $\alpha_1\alpha_6\beta_{2/3}\gamma_2$, $\alpha_6\beta_{2/3}\gamma_2$, or $\alpha_{1/6}\beta_{2/3}$.

Inhibition vs. excitation of PFs by axonal $GABA_AR$s. In a minority of experiments, we observed an inhibitory effect of GABA photolysis on the volley amplitude. This effect is likely similar to the biphasic effect of GABA on PF excitability in response to pressure pipette application of agonists (Stell 2011). We have found that the inhibition is smaller but otherwise consistent with that described by Stell; in our average data (e.g., Figs. 1*C*, 6*A*, and 7*A*), we also observed excitation followed by inhibition. Inhibition was not caused by $GABA_B$ receptor activation and was not associated with a reduction in conduction velocity. In a minority of experiments, inhibition could be observed in the absence of excitation; it also appeared to decrease with age (Fig. 3). The observations that inhibition develops more slowly than excitation and that it is more prominent under conditions in which receptors are strongly activated suggest that inhibition may result from shifts in ionic gradients.

PF $GABA_AR$s increase conduction velocity. The reduction in volley latency and increase in the volley velocity seen with $GABA_A$R activation in PFs in both our experiments and our model are reflective of a phenomenon termed "supernormal excitability" (Gardner-Medwin 1972). Increases in PF volley amplitudes were seen in response to trains of stimuli in vivo and were accompanied by 10–20% increases in conduction velocity, similar to that described here. Subsequent work suggested that potassium accumulation might play a role (Malenka et al. 1981, 1983), however, the constraints of studying the phenomenon in vivo made it difficult to dissect the underlying mechanisms.

Our observations suggest that excitatory $GABA_A$Rs on PF axons may contribute to supernormal excitability. On the basis of our experiments, we cannot rule out the possibility that potassium accumulation could contribute to supernormal excitability, as well; indeed, the computational model shows that

any modest depolarization from the axonal resting potential by a few millivolts will speed conduction velocity.

Why then does this not occur in all axon types? A key determinate in our model of whether depolarization leads to axon excitability are the properties of voltage-gated sodium conductance, particularly the voltage dependence of inactivation (the h∞ curve for a Hodgkin Huxley-type channel). We found that velocity increases were opposed by sodium channel inactivation at depolarized potentials. When the h∞ curve was shifted to negative potentials, reduced sodium channel availability at depolarized potentials mitigated the increase in axon excitability. In this regard it is intriguing to note that both calyx of Held (Kim et al. 2010) and cerebellar granule cells (Afshari et al. 2004) express an unusual form of voltage-gated sodium current characterized by a resurgent activation behavior, a persistent sodium current fraction, and a right-shifted availability (h∞) curve (Bant and Raman 2010). This current is mediated by the interaction between $Na_V1.6$, a pore-forming voltage-gated sodium channel subunit, and an accessory subunit, $\beta 4$ (Grieco et al. 2005). Knockdown of the $\beta 4$-subunit in cerebellar granule cells leads to a leftward shift of the sodium current inactivation curve (Bant and Raman 2010), indicating that the resurgent gating mechanism is accompanied by an increased steady-state availability of sodium channels at membrane potentials in the critical potential range between the resting potential and spike threshold. These results raise the interesting possibility that this specialized voltage-gated sodium current may be an important determinant of whether axonal depolarization is coupled to increased conduction velocity in axons.

Conclusion. With the use of extracellular field recordings of evoked population APs, our data confirm a robust excitatory effect of GABA on PFs that had been observed with calcium imaging and single-neuron electrophysiological approaches (Pugh and Jahr 2011; Stell 2011; Stell et al. 2007). Use of subunit-specific pharmacology and knockout animals suggests that δ-subunit-containing $GABA_AR$ subtypes play a minor role in these effects and that they are likely mediated by α_6- and γ_2-containing $GABA_ARs$. We also report that activation of axonal $GABA_ARs$ can increase AP conduction velocity. Endogenous GABA release mimics the excitatory effect consistent with a physiological role. A simplified NEURON model recapitulates our experimental findings and suggests that the excitatory effect will be sensitive to specific features of voltage-gated sodium channels such as the voltage dependence of availability. Through these physiological actions, PF $GABA_ARs$ may exert an important role in signal processing of sensorimotor information in the granule cell layer.

ACKNOWLEDGMENTS

We are grateful to Vivy Tran for technical support and Dr. Walther Akemann for initial assistance in construction of the computational model.

GRANTS

This work was supported by National Institutes of Health Grants AA19737 (to T. S. Otis), T32NS007101 (to S. S. Dellal), and T32NS058280 (to R. Luo).

DISCLOSURES

T. S. Otis is an associate editor for the *Journal of Neurophysiology*.

AUTHOR CONTRIBUTIONS

Author contributions: S.S.D., R.L., and T.S.O. conception and design of research; S.S.D. and R.L. performed experiments; S.S.D. and R.L. analyzed data; S.S.D., R.L., and T.S.O. interpreted results of experiments; S.S.D. and R.L. prepared figures; S.S.D., R.L., and T.S.O. drafted manuscript; S.S.D., R.L., and T.S.O. edited and revised manuscript; S.S.D., R.L., and T.S.O. approved final version of manuscript.

REFERENCES

Afshari FS, Ptak K, Khaliq ZM, Grieco TM, Slater NT, McCrimmon DR, Raman IM. Resurgent Na currents in four classes of neurons of the cerebellum. *J Neurophysiol* 92: 2831–2843, 2004.

Alle H, Geiger JR. GABAergic spill-over transmission onto hippocampal mossy fiber boutons. *J Neurosci* 27: 942–950, 2007.

Bant JS, Raman IM. Control of transient, resurgent, and persistent current by open-channel block by Na channel $\beta 4$ in cultured cerebellar granule neurons. *Proc Natl Acad Sci USA* 107: 12357–12362, 2010.

Belelli D, Lambert JJ, Peters JA, Wafford K, Whiting PJ. The interaction of the general anesthetic etomidate with the gamma-aminobutyric acid type A receptor is influenced by a single amino acid. *Proc Natl Acad Sci USA* 94: 11031–11036, 1997.

Belenky MA, Sollars PJ, Mount DB, Alper SL, Yarom Y, Pickard GE. Cell-type specific distribution of chloride transporters in the rat suprachiasmatic nucleus. *Neuroscience* 165: 1519–1537, 2009.

Blaesse P, Airaksinen MS, Rivera C, Kaila K. Cation-chloride cotransporters and neuronal function. *Neuron* 61: 820–838, 2009.

Brickley SG, Cull-Candy SG, Farrant M. Development of a tonic form of synaptic inhibition in rat cerebellar granule cells resulting from persistent activation of $GABA_A$ receptors. *J Physiol* 497 753–759, 1996.

Brickley SG, Revilla V, Cull-Candy SG, Wisden W, Farrant M. Adaptive regulation of neuronal excitability by a voltage-independent potassium conductance. *Nature* 409: 88–92, 2001.

Bright DP, Renzi M, Bartram J, McGee TP, MacKenzie G, Hosie AM, Farrant M, Brickley SG. Profound desensitization by ambient GABA limits activation of delta-containing $GABA_A$ receptors during spillover. *J Neurosci* 31: 753–763, 2011.

Chang Y, Xie Y, Weiss DS. Positive allosteric modulation by ultraviolet irradiation on $GABA_A$, but not $GABA_C$, receptors expressed in Xenopus oocytes. *J Physiol* 536: 471–478, 2001.

Clark JA, Deutch AY, Gallipoli PZ, Amara SG. Functional expression and CNS distribution of a beta-alanine-sensitive neuronal GABA transporter. *Neuron* 9: 337–348, 1992.

DiGregorio DA, Rothman JS, Nielsen TA, Silver RA. Desensitization properties of AMPA receptors at the cerebellar mossy fiber granule cell synapse. *J Neurosci* 27: 8344–8357, 2007.

Dittman JS, Regehr WG. Mechanism and kinetics of heterosynaptic depression at a cerebellar synapse. *J Neurosci* 17: 9048–9059, 1997.

Diwakar S, Magistretti J, Goldfarb M, Naldi G, D'Angelo E. Axonal Na^+ channels ensure fast spike activation and back-propagation in cerebellar granule cells. *J Neurophysiol* 101: 519–532, 2009.

Durkin MM, Smith KE, Borden LA, Weinshank RL, Branchek TA, Gustafson EL. Localization of messenger RNAs encoding three GABA transporters in rat brain: an in situ hybridization study. *Brain Res Mol Brain Res* 33: 7–21, 1995.

Eccles JC, Schmidt R, Willis WD. Pharmacological Studies on Presynaptic Inhibition. *J Physiol* 168: 500–530, 1963.

Farrant M, Nusser Z. Variations on an inhibitory theme: phasic and tonic activation of $GABA_A$ receptors. *Nat Rev Neurosci* 6: 215–229, 2005.

Gardner-Medwin AR. An extreme supernormal period in cerebellar parallel fibres. *J Physiol* 222: 357–371, 1972.

Glickfeld LL, Roberts JD, Somogyi P, Scanziani M. Interneurons hyperpolarize pyramidal cells along their entire somatodendritic axis. *Nat Neurosci* 12: 21–23, 2009.

Grieco TM, Malhotra JD, Chen C, Isom LL, Raman IM. Open-channel block by the cytoplasmic tail of sodium channel $\beta 4$ as a mechanism for resurgent sodium current. *Neuron* 45: 233–244, 2005.

Hodgkin AL, Huxley AF. A quantitative description of membrane current and its application to conduction and excitation in nerve. *J Physiol* 117: 500–544, 1952.

Jechlinger M, Pelz R, Tretter V, Klausberger T, Sieghart W. Subunit composition and quantitative importance of hetero-oligomeric receptors: $GABA_A$ receptors containing $\alpha 6$ subunits. *J Neurosci* 18: 2449–2457, 1998.

Kaneko H, Putzier I, Frings S, Kaupp UB, Gensch T. Chloride accumulation in mammalian olfactory sensory neurons. *J Neurosci* 24: 7931–7938, 2004.

Khirug S, Yamada J, Afzalov R, Voipio J, Khiroug L, Kaila K. GABAergic depolarization of the axon initial segment in cortical principal neurons is caused by the Na-K-2Cl cotransporter NKCC1. *J Neurosci* 28: 4635–4639, 2008.

Kim JH, Kushmerick C, von Gersdorff H. Presynaptic resurgent Na^+ currents sculpt the action potential waveform and increase firing reliability at a CNS nerve terminal. *J Neurosci* 30: 15479–15490, 2010.

Li B, McKernan K, Shen W. Spatial and temporal distribution patterns of Na-K-2Cl cotransporter in adult and developing mouse retinas. *Vis Neurosci* 25: 109–123, 2008.

Malenka RC, Kocsis JD, Ransom BR, Waxman SG. Modulation of parallel fiber excitability by postsynaptically mediated changes in extracellular potassium. *Science* 214: 339–341, 1981.

Malenka RC, Kocsis JD, Waxman SG. The supernormal period of the cerebellar parallel fibers effects of $[Ca^{2+}]_o$ and $[K^+]_o$. *Pflügers Arch* 397: 176–183, 1983.

Meera P, Olsen RW, Otis TS, Wallner M. Etomidate, propofol and the neurosteroid THDOC increase the GABA efficacy of recombinant $\alpha4\beta3\delta$ and $\alpha4\beta3$ $GABA_A$ receptors expressed in HEK cells. *Neuropharmacology* 56: 155–160, 2009.

Meera P, Wallner M, Otis TS. Molecular basis for the high THIP/gaboxadol sensitivity of extrasynaptic $GABA_A$ receptors. *J Neurophysiol* 106: 2057–2064, 2011.

Mikawa S, Wang C, Shu F, Wang T, Fukuda A, Sato K. Developmental changes in KCC1, KCC2 and NKCC1 mRNAs in the rat cerebellum. *Brain Res Dev Brain Res* 136: 93–100, 2002.

Mohler H, Crestani F, Rudolph U. $GABA_A$-receptor subtypes: a new pharmacology. *Curr Opin Pharmacol* 1: 22–25, 2001.

Mortensen M, Smart TG. Extrasynaptic alphabeta subunit $GABA_A$ receptors on rat hippocampal pyramidal neurons. *J Physiol* 577: 841–856, 2006.

Nusser Z, Sieghart W, Somogyi P. Segregation of different $GABA_A$ receptors to synaptic and extrasynaptic membranes of cerebellar granule cells. *J Neurosci* 18: 1693–1703, 1998.

Pirker S, Schwarzer C, Wieselthaler A, Sieghart W, Sperk G. $GABA_A$ receptors: immunocytochemical distribution of 13 subunits in the adult rat brain. *Neuroscience* 101: 815–850, 2000.

Price GD, Trussell LO. Estimate of the chloride concentration in a central glutamatergic terminal: a gramicidin perforated-patch study on the calyx of Held. *J Neurosci* 26: 11432–11436, 2006.

Pugh JR, Jahr CE. Axonal $GABA_A$ receptors increase cerebellar granule cell excitability and synaptic activity. *J Neurosci* 31: 565–574, 2011.

Rudomin P, Schmidt RF. Presynaptic inhibition in the vertebrate spinal cord revisited. *Exp Brain Res* 129: 1–37, 1999.

Ruiz A, Campanac E, Scott RS, Rusakov DA, Kullmann DM. Presynaptic $GABA_A$ receptors enhance transmission and LTP induction at hippocampal mossy fiber synapses. *Nat Neurosci* 13: 431–438, 2010.

Ruiz A, Fabian-Fine R, Scott R, Walker MC, Rusakov DA, Kullmann DM. $GABA_A$ receptors at hippocampal mossy fibers. *Neuron* 39: 961–973, 2003.

Sabatini BL, Regehr WG. Control of neurotransmitter release by presynaptic waveform at the granule cell to Purkinje cell synapse. *J Neurosci* 17: 3425–3435, 1997.

Santhakumar V, Hanchar HJ, Wallner M, Olsen RW, Otis TS. Contributions of the $GABA_A$ receptor $\alpha6$ subunit to phasic and tonic inhibition revealed by a naturally occurring polymorphism in the $\alpha6$ gene. *J Neurosci* 26: 3357–3364, 2006.

Schmid G, Bonanno G, Raiteri L, Sarviharju M, Korpi ER, Raiteri M. Enhanced benzodiazepine and ethanol actions on cerebellar $GABA_A$ receptors mediating glutamate release in an alcohol-sensitive rat line. *Neuropharmacology* 38: 1273–1279, 1999.

Seja P, Schonewille M, Spitzmaul G, Badura A, Klein I, Rudhard Y, Wisden W, Hubner CA, De Zeeuw CI, Jentsch TJ. Raising cytosolic Cl^- in cerebellar granule cells affects their excitability and vestibulo-ocular learning. *EMBO J* 31: 1217–1230, 2012.

Shu HJ, Bracamontes J, Taylor A, Wu K, McCollum M, Akk G, Manion B, Evers AS, Krishnan K, Covey DF, Zorumski CF, Steinbach JH, Mennerick S. Characteristics of concatemeric $GABA_A$ receptors containing $\alpha4/\delta$ subunits expressed in Xenopus oocytes. *Br J Pharmacol* 165: 2228–2243, 2012.

Stell BM. Biphasic action of axonal GABA-A receptors on presynaptic calcium influx. *J Neurophysiol* 105: 2931–2936, 2011.

Stell BM, Brickley SG, Tang CY, Farrant M, Mody I. Neuroactive steroids reduce neuronal excitability by selectively enhancing tonic inhibition mediated by δ subunit-containing $GABA_A$ receptors. *Proc Natl Acad Sci USA* 100: 14439–14444, 2003.

Stell BM, Rostaing P, Triller A, Marty A. Activation of presynaptic $GABA_A$ receptors induces glutamate release from parallel fiber synapses. *J Neurosci* 27: 9022–9031, 2007.

Szabadics J, Varga C, Molnar G, Olah S, Barzo P, Tamas G. Excitatory effect of GABAergic axo-axonic cells in cortical microcircuits. *Science* 311: 233–235, 2006.

Trigo FF, Chat M, Marty A. Enhancement of GABA release through endogenous activation of axonal $GABA_A$ receptors in juvenile cerebellum. *J Neurosci* 27: 12452–12463, 2007.

Turecek R, Trussell LO. Reciprocal developmental regulation of presynaptic ionotropic receptors. *Proc Natl Acad Sci USA* 99: 13884–13889, 2002.

Vranesic I, Iijima T, Ichikawa M, Matsumoto G, Knopfel T. Signal transmission in the parallel fiber-Purkinje cell system visualized by high-resolution imaging. *Proc Natl Acad Sci USA* 91: 13014–13017, 1994.

Wafford KA, van Niel MB, Ma QP, Horridge E, Herd MB, Peden DR, Belelli D, Lambert JJ. Novel compounds selectively enhance delta subunit containing $GABA_A$ receptors and increase tonic currents in thalamus. *Neuropharmacology* 56: 182–189, 2009.

Wang XJ, Liu Y, Sanchez-Vives MV, McCormick DA. Adaptation and temporal decorrelation by single neurons in the primary visual cortex. *J Neurophysiol* 89: 3279–3293, 2003.

Woodruff AR, Monyer H, Sah P. GABAergic excitation in the basolateral amygdala. *J Neurosci* 26: 11881–11887, 2006.

Xiao C, Zhou C, Li K, Ye JH. Presynaptic $GABA_A$ receptors facilitate GABAergic transmission to dopaminergic neurons in the ventral tegmental area of young rats. *J Physiol* 580: 731–743, 2007.

Zhang SJ, Jackson MB. GABA-activated chloride channels in secretory nerve endings. *Science* 259: 531–534, 1993.

Zhang SJ, Jackson MB. $GABA_A$ receptor activation and the excitability of nerve terminals in the rat posterior pituitary. *J Physiol* 483: 583–595, 1995.